Eur. J. Wood Prod. (2016) 74:49–56
DOI 10.1007/s00107-015-0969-y

ORIGINAL

Needle fir wood modified by surface densification and thermal post-treatment: hygroscopicity and swelling behavior

Jian-feng Zhan[1] · **Stavros Avramidis**[2]

Received: 22 December 2014 / Published online: 1 October 2015

Abstract Needle fir (*Abies nephrolepis*) wood was surface densified at two compression ratios (16.1 and 21.7 %), two hot-pressing temperatures (160 and 180 °C) for a pressure holding duration of 10 min. Subsequently, it was thermally treated at two temperatures (180 and 200 °C) for 1 h. The equilibrium moisture content responses and radial swelling strain ratios were calculated for thirteen types of adsorption specimens under adsorption and water soaking, respectively. Compared with untreated (control) specimens and densified but non-thermally treated ones, the hygroscopicity of thermally post-treated specimens was significantly decreased. Both hot-pressing temperature and compression ratio showed insignificant influence on the hygroscopicity of all treated specimens. Under the current test conditions, with the increase of thermal post-treatment temperature and the decrease of compression ratio among the thermally post-treated specimens, the radial swelling deformation was significantly decreased. The impact of increasing hot-pressing temperature on the radial swelling was insignificant according to the statistical analysis.

1 Introduction

Needle fir (*Abies nephrolepis*) is a widely distributed plantation wood species in China's North and Northeast regions that has relatively low density and mechanical strength, light color and less appealing grain, attributes that limit its use in furniture, wooden floorings and other value-added markets. Recently, several hydro-thermo-mechanical treatment processes have been developed to modify and improve the properties of low-quality softwood and plantation wood species (Kutnar et al. 2009, 2012; Ding et al. 2011; Kutnar and Kamke 2012a, b; Cai et al. 2012, 2013; Hill et al. 2012; Laine et al. 2013a, b; Zhan et al. 2015). Among them, the combination of surface densification and thermal post-treatment is a promising technology which results in excellent dimensional stability, appealing color and luster, and an increase in selected mechanical properties (Kutnar et al. 2009, 2012; Kutnar and Kamke 2012a, b; Cai et al. 2012, 2013; Hill et al. 2012; Laine et al. 2013a, b; Zhan et al. 2015).

By compressing wood in the transverse direction under specified heat and moisture conditions, wood surface densification aims to improve wood mechanical properties without adding chemical additives (Laine et al. 2013a). Furthermore, fixing the compression-set of densified wood and reducing its recovery and dimensional instability, several thermo-hydro treatments under high temperature have been proven viable and efficient (Cai et al. 2012, 2013; Laine et al. 2013a; Zhan et al. 2015).

High temperature hydro-thermally treated wood exhibits enhanced anti-weathering resistance and improved dimensional stability (Laine et al. 2013b; Todaro et al. 2012; Borrega and Kärenlampi 2010; Gündüz et al. 2008; Gündüz and Aydemir 2009; Tu et al. 2010; Rautkari et al. 2014), which is a matter of great significance for indoor applications such as floor heating, kitchen furnishing, and interiors of bathrooms and saunas. Several researches have investigated the environmental stability of heat-treated wood including solid timber (softwood and hardwood), rotary-peeled veneer and composites (Frühwald 2007;

✉ Jian-feng Zhan
zhanjianfeng2002@sina.com.cn

[1] College of Material Science and Engineering, Northeast Forestry University, Harbin, People's Republic of China

[2] Department of Wood Science, University of British Columbia, Vancouver, BC, Canada

Chaouch et al. 2013; Sik et al. 2010; Liu et al. 2013; Bonigut et al. 2014). The main variables studied included maximum temperatures, holding time at maximum temperature, heating medium and its pressure, heating rate, total processing durations, specimen dimensions (especially thickness), initial moisture content, wood species, etc. (Laine et al. 2013a; Cai et al. 2013; Zhan et al. 2015). During heat treatment, chemical degradation of wood occurs first in hemicelluloses and then in cellulose and lignin (Kamdem et al. 2002). Because of the decrease of hydrophilic hydroxyl groups, wood becomes more stable both dimensionally and biologically. Concurrently, there are also changes in physical properties as a result of the chemical degradation in the wood structure. In general, as the heat treatment temperature rises and the heating duration increases, mass loss increases and thus, density and mechanical strength tend to decrease (Laine et al. 2013a; Cai et al. 2013; Zhan et al. 2015; Tjeerdsma et al. 1998).

Although numerous studies about the physical properties of heat-treated softwood and hardwood species have appeared in the literature (Ding et al. 2011; Todaro et al. 2012; Borrega and Kärenlampi 2010; Gündüz et al. 2008; Gündüz and Aydemir 2009; Tu et al. 2010; Kamdem et al. 2002; Tjeerdsma et al. 1998), a relatively small number have focused on the enhanced environmental durability of surface densified wood products modified by further thermal treatment (Hill et al. 2012; Cai et al. 2012, 2013; Laine et al. 2013b; Welzbacher et al. 2008; Gong et al. 2010). Cai et al. (2012) suggested that the optimized technical parameters were a 25 % compression ratio plus hot-pressing temperature of 170 °C for the densification process, and a temperature of 200 °C plus duration of 3.5 h for a thermal post-treatment. Gong et al. (2010) investigated the interactive effect of surface densification and post-heat-treatment on aspen where the heat-treatment significantly improved the dimensional stability of the surface densified aspen. Laine et al. (2013b) measured the swelling behavior and compression set-recovery of densified and thermally modified Scots pine wood under changing moisture content. Four different methods were applied to untreated, thermally modified, densified and densified plus thermally modified sapwood samples. The progress and extent of thickness set-recovery are significantly dependent upon the conditions where the set-recovery is induced. During wood surface densification process, only few millimeters beneath the surface are compressed under high temperature (140–170 °C) and moist conditions (Laine et al. 2013a; Zhan et al. 2015; Welzbacher et al. 2008; Gong et al. 2010). The surface densified wood must undergo a further thermal post-treatment in order for the compressive deformation accumulated during hot-pressing process is fixed effectively (Welzbacher et al. 2008). Actually, it is the first few cell layers that have been heat-treated almost twice during this whole combined process.

The aim of this study was to investigate the hygroscopicity and thickness swelling behavior in the radial direction of the surface-densified and post-thermally treated wood in relation to the thermal post-treatment temperature and surface compression ratio. Furthermore, the relative contributions of both surface hot-pressing and post thermal treatment to the improved dimensional stability were analyzed in relation to the maximum temperature reached both in the densification and thermal post-treatment process.

2 Materials and methods

2.1 Surface densification and thermal post-treatment

Air-dried needle fir lumber pieces of 4 m long, 250 mm wide (tangential direction) and 35 mm thick (radial direction) were used in this study. The lumber was sourced from Yichun, China, with an average basic density of 319 kg/m^3. After being stored inside a conditioning chamber for more than 1 year at temperature of 20–24 °C and relative humidity (RH) of 55–60 % that resulted in an equilibrium moisture content (EMC) of 12 ± 2 %, they were then cut into 160 mm long and 60 mm wide samples that were planed to two thicknesses, namely, 28 and 30 mm. The samples that did not have any visual defect, were selected as the specimens for the hot-pressing and post-thermal modification study.

Abies nephrolepis sapwood lumbers were compressed radially in an open hot press for wooden composites. After placing the samples in the press, the hot-pressing machine was closed with a constant speed to prevent drying of the samples before compression. The target thickness of densified board was controlled with two metal stackers. The samples were held under compression between two electrically heated metal plates at the target temperature for 10 min, after which the system was allowed to cool down for 2 h, to a temperature below 100 °C. With the two initial specimen thicknesses (28 and 30 mm) and a target thickness of 23.5 mm in hot-pressing, the compression ratios of 16.1 and 21.7 %, respectively, were evaluated. Two hot-pressing temperatures, namely 160 and 180 °C, were used for the surface densification process. In order to fix the compressive sets, half of these surface densified specimens were placed into a laboratory thermal modification oven. The specimens were first oven-dried at 103 ± 2 °C for 1 h and then heated to the target temperature within 1 h. Two treatment temperatures, namely, 180 and 200 °C, were utilized, with a holding duration of 1 h. During the heating

process and thermal treatment stage, steam injection was utilized inside the oven chamber, acting as protecting media. The average weight loss of the thermally post-treated samples was 0.5 and 1.45 % for the target temperature 180 and 200 °C, respectively. The more detailed processing steps of the surface densification and thermal post-treatment are discussed in Zhan et al. (2015).

2.2 Adsorption specimens preparation

After surface densification and thermal post-treatment, half of these lumber pieces were selected for the adsorption tests and were further cut into 50 mm (length), 60 mm (tangential), with actual hot-pressed thickness specimens. With two compression ratios (16.1 and 21.7 %), two surface densification temperatures (160 and 180 °C), two types of post-thermal modification tests (180 and 200 °C) plus the non-heat-treatment, twelve types of specimens were created. Furthermore, in order to gain a comprehensive understanding of the relative contribution of both the surface densification and thermal post-treatment to the wood dimensional stability, an additional type of specimen, namely the non-surface-densified plus non-heat-treated one was chosen as the control that was 50 mm in the longitudinal, 60 mm in the tangential, and 30 mm in the radial direction. The specimen coding scheme used is listed in Table 1.

For each specimen type, there were twelve pieces (replications) selected without any visual defects. Altogether, $12 \times 13 = 156$ specimens were used in this adsorption test, which were stored at 24 ± 2 °C and 50 ± 5 % RH for 10 months.

2.3 Adsorption test procedure

Three straight lines were drawn on the four surfaces of each specimen so that the swelling measurements could be determined. For each specimen, the actual swelling deformation can be measured at six specific positions. For instance, the distance between 1 and 1^* is for the position one (Fig. 1). All specimens were weighed in advance and

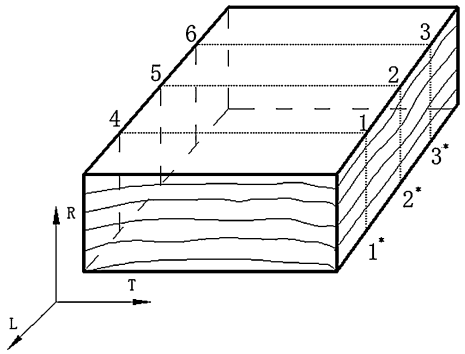

Fig. 1 Radial swelling measure points

their initial thicknesses were measured with a pair of digital calipers (the average of six positions). Subsequently, they were placed in an oven at 103 ± 2 °C for 24 h and the final weights and dimensions were determined again. The adsorption test was carried out in a GDS Environmental Test Chamber (Xinda Test Equipment Co., LTD, Suzhou, China), with the conditioning temperature accuracy held at ±0.5 °C and RH accuracy at ±3 %. The oven-dried specimens were exposed to five RH levels consecutively, namely, 30, 50, 70, 88, 98 %, with a constant temperature setting at 40 °C. For each adsorption test condition, the individual specimens were conditioned for at least $24 \times 7 = 168$ h, during which they were weighed and their radial dimensions measured periodically until a constant weight was achieved before proceeding to the next adsorption step. At the end of the adsorption cycle, all specimens were taken out and submerged in distilled water until full water saturation and their final weights and dimension were re-measured.

The EMC at the end of each adsorption test for post-thermally treated, non-thermally treated and control specimens were calculated as:

$$EMC = \frac{(W_e - W_o)}{W_o} \times 100\,\% \quad (1)$$

where W_o is the oven-dried weight of each specimen and W_e is the specimen weight at equilibrium.

Table 1 Nomenclature of test specimens

Nomenclature	Contents represented
Control	Non-surface-densified and non-post-thermal treated, initial thickness 30 mm
28	Initial thickness 28, compression ratio 16.1 %
30	Initial thickness 30, compression ratio 21.7 %
160	Hot-pressing temperature 160 °C, processing duration 10 min
180	Hot-pressing temperature 180 °C, processing duration 10 min
H1	Thermal post-treatment temperature 180 °C, processing duration 1 h
H2	Thermal post-treatment temperature 200 °C, processing duration 1 h
NH	Without thermal post-treatment

2.4 Swelling strain ratio S_r

For the purpose of quantitatively analyzing the thickness swelling behavior under consecutive adsorption tests, a non-dimensional swelling strain ratio S_r was defined as

$$S_r = \frac{(\ell - \ell_o)}{\ell_s} \times 100\,\% \quad (2)$$

where ℓ_o is the oven-dried thickness (mm) of the specified adsorption specimens, in the radial direction. ℓ_s equals the final water saturated dimension and ℓ is the actual thickness dimension determined under each adsorption equilibrium state.

3 Results and discussions

3.1 EMC responses

In order to show the effect of the combined modification treatment on the EMC explicitly, these thirteen types of specimens were divided into four groups based on the initial thickness and hot-pressing temperature, shown in Tables 2 and 3, respectively.

Under constant temperature of 40 °C and five relative humidities used, the average EMC values of the control specimens were 4.07, 7.12, 9.94, 14.80 and 20.27 %, respectively. The adsorption isotherm curve and its Hailwood-Horrobin model regression are plotted in Fig. 2. For comparison purposes, the adsorption isotherm data of fir control specimens (Gündüz et al. 2008) at 20 °C are also presented herein, both of which show a sigmoid shape. According to Fig. 2, as the temperature increases from 20 to 40 °C, the adsorption isotherm and its fitting curves move towards the x-axis, which was well predicted by "three-variable models" proposed by Avramidis (1989).

According to Fig. 3a–d, as well as Tables 2 and 3, the hygroscopicity of surface-densified specimens was decreased due to the thermal post-treatment, especially under high humidity conditions. For instance, in Table 2, compared with the controls at 50 % RH, the reduction of EMC values for the NH-160-28, H1-160-28 and H2-160-28 were 8, 9 and 14 %, respectively. The EMC differences between the controls and the thermally post-treated specimens widened as the target RH values increased. This phenomenon was also discovered by Gündüz et al. (2008).

A reusable two-factor analysis of variance (ANOVA) was performed based on the relationship between the EMC responses and thermal post-treatment factors. According to the statistic examination, the EMC responses for all kinds of adsorption specimens were significantly affected by the thermal post-treatment ($p = 0$). An insignificant decrease of the EMC response for all kinds of adsorption specimens was found when the hot-pressing temperature increased from 160 to 180 °C ($p = 0.91$). Same response was observed when the compression ratio increased from 16.1 to 21.7 % ($p = 0.29$).

Table 2 EMC (%) of specimens (28 mm) at different relative humidity levels (standard deviation)

Relative humidity (%)	30	50	70	88	98
H2-160-28	3.40 (0.10)	6.09 (0.17)	8.70 (0.17)	12.45 (0.30)	17.47 (0.56)
H1-160-28	3.76 (0.07)	6.48 (0.18)	9.35 (0.14)	13.34 (0.34)	19.19 (0.64)
NH-160-28	3.70 (0.04)	6.52 (0.16)	9.43 (0.10)	13.48 (0.11)	19.18 (0.17)
H2-180-28	3.43 (0.16)	6.03 (0.29)	8.83 (0.36)	12.43 (0.36)	17.33 (0.74)
H1-180-28	3.76 (0.08)	6.60 (0.28)	9.19 (0.15)	13.36 (0.15)	18.87 (0.35)
NH-180-28	3.72 (0.10)	6.52 (0.19)	9.44 (0.15)	13.54 (0.18)	18.82 (0.31)
Control	4.07 (0.08)	7.12 (0.26)	9.94 (0.20)	14.80 (0.16)	20.27 (0.18)

Table 3 EMC (%) of specimens (30 mm) at different relative humidity levels (standard deviation)

Relative humidity (%)	30	50	70	88	98
H2-160-30	3.20 (0.07)	6.36 (0.21)	8.73 (0.10)	12.52 (0.15)	17.51 (0.21)
H1-160-30	3.69 (0.04)	6.49 (0.15)	9.25 (0.07)	13.37 (0.11)	19.12 (0.19)
NH-160-30	3.99 (0.11)	6.89 (0.20)	9.78 (0.08)	13.95 (0.12)	19.48 (0.28)
H2-180-30	3.45 (0.08)	5.91 (0.25)	8.69 (0.15)	12.60 (0.24)	17.74 (0.53)
H1-180-30	3.74 (0.09)	6.56 (0.16)	9.29 (0.19)	13.35 (0.25)	19.32 (0.37)
NH-180-30	3.77 (0.14)	7.00 (0.34)	9.74 (0.21)	13.93 (0.33)	19.43 (0.65)
Control	4.07 (0.08)	7.12 (0.26)	9.94 (0.20)	14.80 (0.16)	20.27 (0.18)

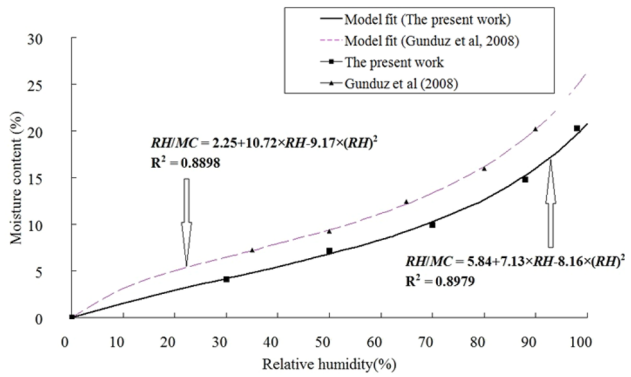

Fig. 2 EMC response and its mathematical fitting curve for two kinds of adsorption tests

3.2 Thickness swelling behavior

The impact of the combinations of the surface densification and thermal post-treatment on thickness swelling strain ratio is shown in Fig. 4a–f for various humidity levels and 96-h water soaking. Compared with the control specimens, the swelling strain ratio of all the post-thermally treated specimens increased under all adsorption states. As the adsorption test proceeded from one humidity level to next, the differences between the control specimens and post-thermally treated ones widened accordingly. For example, the difference between the control and specimen H1-180-30 was 0.43 % for RH 30 %, 0.82 % for RH 50 %, 1.27 % for RH 70 %, 1.9 % for RH 88 %, 3.32 % for RH 98 % and 4.25 % for the water soaked condition, respectively. Nevertheless, the investigation of the swelling behavior between two thermal post-treatment temperature levels showcased a decreasing trend. As the thermal treatment temperature increased from 180 to 200 °C, the swelling strain ratio decreased accordingly. For instance, the difference between the specimen H2-160-28 and H1-160-28 was −0.02 % for RH 30 %, −0.23 % for RH 50, −0.52 % for RH 70 %, −0.94 % for RH 88 %, −1.41 % for RH 98 %, respectively. After statistical examination (two-factor ANOVA), it was found that the thickness swelling behavior along the radial direction was significantly affected by the thermal post-treatment temperature ($p = 0.044$).

It should be noted that all the adsorption specimens had been preserved inside sealed chambers for 10 months, during which the compressive visco-elastic deformation of

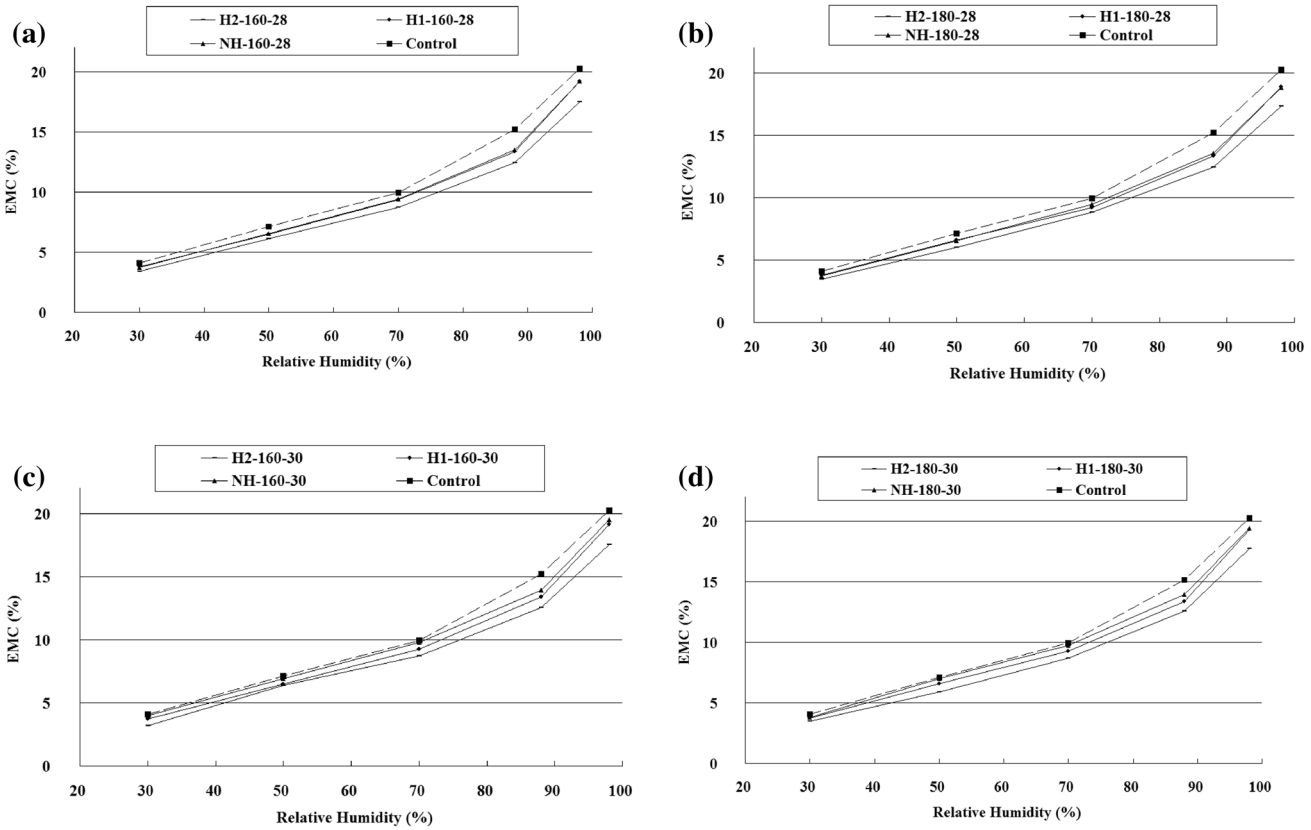

Fig. 3 EMC response for the specimens densified at **a** 160 °C with initial thickness of 28 mm, **b** 180 °C with initial thickness of 28 mm, **c** 160 °C with initial thickness of 30 mm and **d** 180 °C with initial thickness of 30 mm

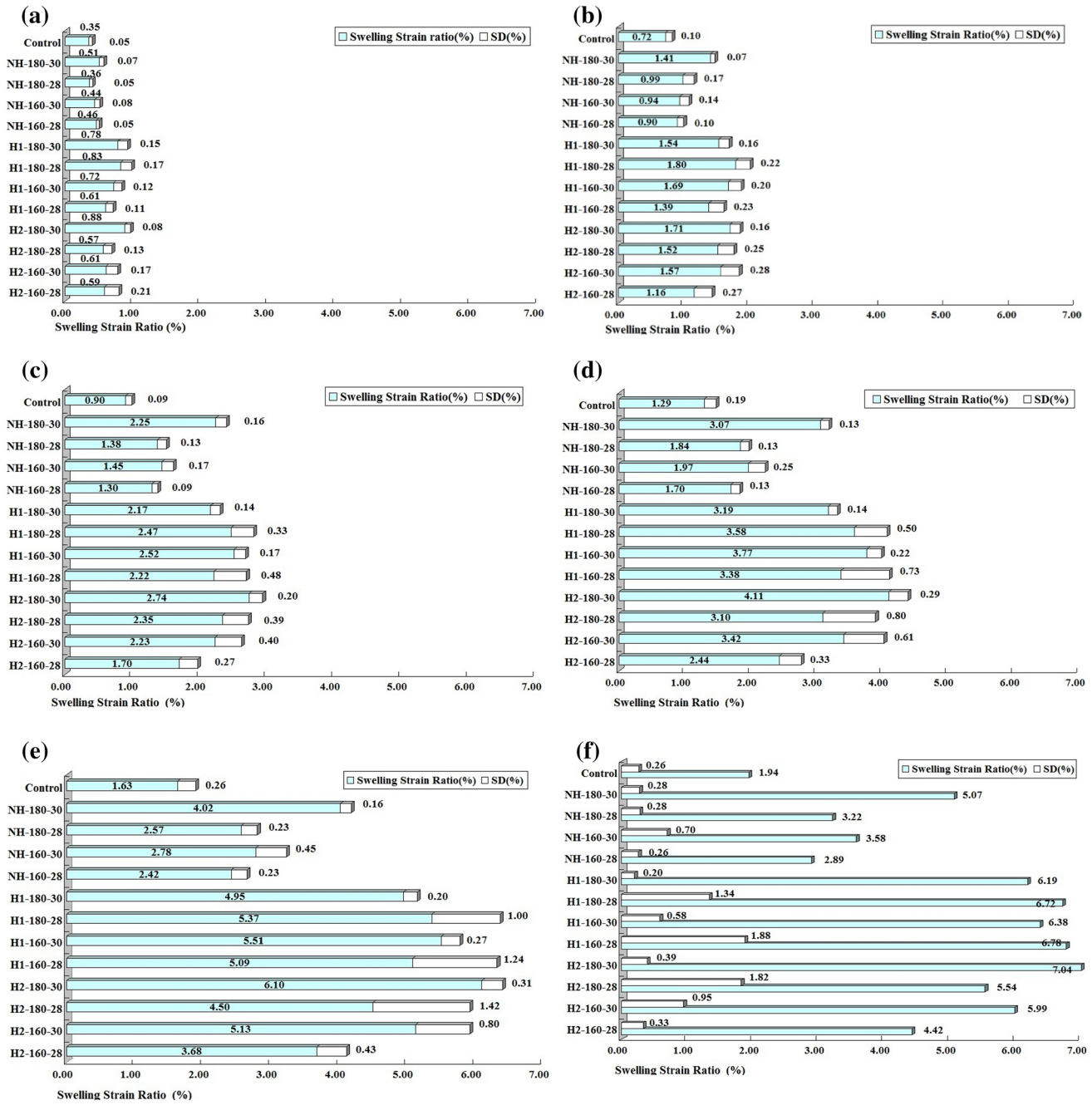

Fig. 4 Thickness swelling behaviors under **a** 30 % RH, **b** 50 % RH, **c** 70 % RH, **d** 88 % RH, **e** 98 % RH and **f** in moisture saturation

the non-thermally treated specimen NH series was released more significantly than that of the post-thermally treated ones. As a consequence, the increase of the swelling strain ratio for the NH series specimens was lower than that of the post-thermally treated ones.

The impact of the hot-pressing temperature on radial swelling was very complicated due to the interactive effect of hot-pressing and thermal post-treatment. The statistical analysis (two-factor ANOVA) showed that the influence of hot-pressing temperature ($p = 0.131$) on the radial swelling was insignificant according to Fig. 4a–f. A similar conclusion was also reached by Cai et al. (2013) and Welzbacher et al. (2008) for the maximum swelling of the densified wood.

According to wood visco-elasticity theory (Zhan et al. 2009), with the increase of the compression ratio for densified wood, the resulting dimensional stability would be compromised. The recovery of the compressive deformation along thickness would become more significantly in case of no further treatment that followed. As the

compression ratio increased from 16.1 to 21.7 %, the radial swelling strain ratio of all the specimens (except H1–180) increased correspondingly. According to statistical analysis (two-factor ANOVA, $p = 0.04$), a significant reduction in the radial swelling deformation could be achieved by the decrease of compression ratio from 21.7 to 16.1 %. A research by Cai et al. (2013) also showed the same trend between the water-soaked swelling deformation and compression ratio.

4 Conclusion

In the light of this investigation, following conclusions could be drawn:

1. At 40 °C and five relative humidity levels, the hygroscopicity of the surface densified needle fir was significantly decreased, especially between those post-thermally treated specimens series. Under the RH of 98 %, compared with the control specimens, the average decrease ratio of the EMC value for the specimens post-thermally treated at 200 °C was 13.6 %; compared with the non-post-thermally treated specimens, the average decrease rate of the EMC value for the 200 °C post-thermally treated series was 8.9 %; compared with the specimens post-thermally treated at 180 °C, this parameter became 8.4 %.
2. Compared with the series post-thermally treated at 180 °C, under 40 °C and five targeted RH plus water soaked conditions, the average radial swelling strain ratio of the 200 °C post-thermally treated series decreased significantly, highlighting the improved deformation stability due to the thermal post-treatment of 200 °C plus 1 h duration. The thermal post-treatment temperature significantly affected the radial swelling behavior of the densified needle fir.
3. The increase of the compression ratio from 16.1 to 21.7 % resulted in a significant rise of the radial swelling deformation among the densified specimens, including both non-thermally treated and post-thermally treated one. However, the increase of compression ratios showed no significant effect on the EMC responses of adsorption test specimens.

The combination of surface densification and thermal post-treatment is a promising technology, which can be used to process the plantation needle fir into value-added products with improved dimensional stability, excellent surface properties, and extended application fields.

Acknowledgments This research was financially supported by the Fundamental Research Funds for the Central Universities of China (Northeast Forestry University, No. DL13CB17).

References

Avramidis S (1989) Evaluation of "three-variable" models for the prediction of equilibrium moisture content in wood. Wood Sci Technol 23(3):251–258

Bonigut J, Krug D, Stuckenberg P (2014) Dimensional stability and irreversible thickness swell of thermally treated oriented strandboards (OSB). Eur J Wood Prod 72(5):593–599

Borrega M, Kärenlampi PP (2010) Hygroscopicity of heat-treated Norway spruce (*Picea abies*) wood. Eur J Wood Prod 68(2):233–235

Cai JB, Ding T, Yang L, Yang X (2012) Effect of heat treatment and densification on dimension stability of Poplar wood (in Chinese). China Wood Ind 26(5):41–44

Cai JB, Yang X, Cai LP, Shi (2013) Impact of the combination of densification and thermal modification on dimensional stability and hardness of poplar lumber. Drying Technol 31(10):1107–1113

Chaouch M, Dumarcay S, Petrissans A, Gerardin P (2013) Effect of heat treatment intensity on some conferred properties of different European softwood and hardwood species. Wood Sci Technol 47(4):663–673

Ding T, Gu LB, Li T (2011) Influence of steam pressure on physical and mechanical properties of heat-treated Mongolian pine lumber. Eur J Wood Prod 69(1):121–126

Frühwald E (2007) Effect of high-temperature drying on properties of Norway spruce and larch. Holz Roh Werkst 65(6):411–418

Gong M, Lamason C, Li L (2010) Interactive effect of surface densification and post-heat-treatment on aspen wood. J Mater Process Technol 210(2):293–296

Gündüz G, Aydemir D (2009) Some physical properties of heat-treated hornbeam (*Carpinus betulus* L.) wood. Drying Technol 27(5):714–720

Gündüz G, Niemz P, Aydemir D (2008) Changes in specific gravity and equilibrium moisture content in heat-treated fir (*Abies nordmanniana* subsp. bornmülleriana Mattf.) Wood. Drying Technol 26(9):1135–1139

Hill CAS, Ramsay J, Keating B, Laine K, Rautkari L, Hughes M, Constant B (2012) The water vapour sorption properties of thermally modified and densified wood. J Mater Sci 47(7):3191–3197

Kamdem DP, Pizzi A, Jermannaud A (2002) Durability of heat treated wood. Holz Roh Werkst 60(1):1–6

Kutnar A, Kamke FA (2012a) Influence of temperature and steam environment on set recovery of compressive deformation of wood. Wood Sci Technol 46(5):953–964

Kutnar A, Kamke FA (2012b) Compression of wood under saturated steam, superheated steam, and transient conditions at 150, 160 and 170 °C. Wood Sci Technol 46(1–3):73–88

Kutnar A, Kamke FA, Sernek M (2009) Density profile and morphology of viscoelastic thermal compressed wood. Wood Sci Technol 43(1–2):57–68

Kutnar A, Rautkari L, Laine K, Hughes M (2012) Thermodynamic characteristics of surface densified solid Scots pine wood. Eur J Wood Prod 70(5):727–734

Laine K, Rautkari L, Hughes M, Kutnar A (2013a) Reducing the set-recovery of surface densified solid Scots pine wood by hydrothermal post-treatment. Eur J Wood Prod 71(1):17–23

Laine K, Belt T, Rautkari L, Ramsay J, Hill CAS, Hughes M (2013b) Measuring the thickness swelling and set-recovery of densified and thermally modified Scots pine solid wood. J Mater Sci 48(24):8530–8538

Liu H, Kamke FA, Guo K (2013) Integrated drying and thermo-hydro-mechanical modification of western hemlock veneer. Eur J Wood Prod 71(2):173–181

Rautkari L, Honkanen J, Hill CAS, Ridley-Ellis D, Hughes M (2014) Mechanical and physical properties of thermally modified Scots pine wood in high pressure reactor under saturated steam at 120, 150 and 180 & #xB0;C. Eur J Wood Prod 72(1):33–41

Sik HS, Choo KT, Zakaria S, Ahmad S, How SS, Chia CH, Yusoff M (2010) Dimensional stability of high temperature-dried rubberwood solid lumber at two equilibrium moisture content conditions. Drying Technol 28(9):1083–1090

Tjeerdsma BF, Boonstra M, Pizzi A, Tekely P, Militz H (1998) Characterisation of thermally modified wood: molecular reasons for wood performance improvement. Holz Roh Werkst 56(3):149–153

Todaro L, Zanuttini R, Scopa A, Moretti N (2012) Influence of combined hydro-thermal treatments on selective properties of Turkey oak (*Quercus cerris* L.) wood. Wood Sci Technol 46(3):563–578

Tu DY, Wang MJ, Gu LB et al (2010) Effect of super high temperature heat treatment on *Fraxinus mandshurica* board's dimension stability (in Chinese). J Nanjing Forest Univ (Natural Science Edition) 34(3):113–116

Welzbacher CR, Wehsener J, Rapp AO, Haller P (2008) Thermo-mechanical densification combined with thermal modification of Norway spruce in industrial scale—Dimensional stability and durability aspects. Holz Roh Werkst 66(1):39–49

Zhan JF, Gu JY, Cai YC (2009) Dynamic visco-elastic characteristics of larch timber during conventional drying process (in Chinese). J Beijing Forest Univ 31(1):129–134

Zhan JF, Cao J, Gu JY et al (2015) Surface-densification and high-temperature hydrothermal post treatment of the *Abies nephrolepis* lumber (in Chinese). J Nanjing Forest Univ (Natural Science Edition) 39(3):119–124